18. For $V(TCNE)_x \cdot yCH_2Cl_2$ a range of $x$ and $y$ is observed for preparations differing in solvents and mole ratios of the starting materials; oxygen and perhaps benzene in small amounts are present in some cases. For the material discussed herein $x \sim 2$ and $y \sim 1/2$. Magnetic materials with $1.5 \leq x \leq 2$ and $0 \leq y \leq 1$ have also been prepared. Elemental analysis: calculated (observed) for $C_{12.5}HClN_8V$: %C = 42.95 (42.81, 43.20, 43.00), %H = 0.29 (0.14, 0.68, 0.35), %N = 32.05 (30.63, 30.00, 31.04), and %V = 14.57 $(15.31)^-$, % chlorine was not reproducible. Trace elements {Fe (41 ppm), Co [none detected (<25 ppm)], Ni [none detected (<50 ppm)], and Cr (34 ppm)] were determined by ICP microanalysis. Thermal decomposition in a mass spectrometer showed the loss of $CH_2Cl_2$ and TCNE.
19. Similar results are obtained with the use of diethyl ether, benzene, 1,2-dichloroethane, and hexane as solvents.
20. M. F. Rettig and R. M. Wing, *Inorg. Chem.* **8**, 2685 (1969).
21. H. Braunwarth, G. Huttner, L. Zsolnai, *J. Organomet. Chem.* **372**, C23 (1989).
22. R. Gross-Lambert, W. Kaim, B. Olbrich-Duessner, *Inorg. Chem.* **29**, 5046 (1990).
23. W. Beck, R. Schlodder, K. H. Lechler, *J. Organomet. Chem.* **54**, 303 (1973); A. Maisonnat, J-J. Bonnet, R. Poilblanc, *Inorg. Chem.* **19**, 3168 (1980); M. I. Bruce, T. W. Hambly, M. R. Snow, A. G. Swincer, *J. Organomet. Chem.* **235**, 105 (1982); A. L. Balch, *J. Am. Chem. Soc.* **98**, 285 (1976); T. S. Janik, K. A. Bernard, M. R. Churchill, J. D. Atwood, *J. Organomet. Chem.* **323**, 247 (1987).
24. J. S. Miller *et al.*, *J. Am. Chem. Soc.* **112**, 381 (1990).
25. In contrast, the reaction of $V(C_6H_6)_2$ with TCNQ, 2,3-dichloro-5,6-dicyanobenzoquinone, hexacyanobutadiene, or 2,3,5,6-tetracyanobenzoquinone leads to precipitates that do not exhibit field-dependent magnetic susceptibilities $\chi$ and as evidenced from the fit of the susceptibility data to the Curie-Weiss expression $[\chi \propto (T - \theta)^{-1}]$, these materials exhibit antiferromagnetic behavior (that is, $\theta < 0$).
26. J. B. Goodenough, *Magnetism and the Chemical Bond* (Wiley-Interscience, New York, 1963), pp. 98, 100, and 104.
27. J. S. Miller and D. A. Dixon, *Science* **235**, 871 (1987).
28. Other less likely possibilities are $S = 1/2$ $V^{IV}$ and $S = 0$ $[TCNE]^{2-}$. Mixed valent formulations, such as $S = 1$ $V^{III}$ and $S = 1/2[TCNE]^{\cdot-}$ and $S = 0$ $[TCNE]^{2-}$, also cannot be ignored.

29. We acknowledge support from the U.S. Department of Energy Division of Materials Science grant DE-FG02-86ER45271.A000. We appreciate the EPR spectra provided by S. Hill and P. J. Krusic, XPS spectra determined by J. Wyre and G. Blackman, powder diffraction taken by G. Hyatt, C. M. Foris, and K. H. Gardner, IR spectra by A. P. Berry, synthetic assistance by C. Vazquez and S. Riggs, energy dispersive x-ray analysis by M. Harmer, hysteresis data taken by M. H. Reilly, P. F. Carcia, and K. S. Narayan, helpful discussions with D. A. Dixon, and ICP microanalysis by T. S. Connell and B. F. Burgess, Jr., Contribution no. 5228 of Central Research & Development, Du Pont.

24 April 1991; accepted 2 May 1991

---

# Electronic States of $K_xC_{60}$: Insulating, Metallic, and Superconducting Character

P. J. BENNING, JOSÉ LUÍS MARTINS, J. H. WEAVER,
L. P. F. CHIBANTE, R. E. SMALLEY

**The recent report of electrical conductivity in the alkali metal fullerides and the discovery of superconductivity at 18 K for $K_xC_{60}$ has raised fundamental questions about the electronic states on either side of the Fermi level, their occupancy with K intercalation, and the mechanism of superconductivity. Direct photoemission evidence is presented of filling of bands derived from the lowest unoccupied molecular orbital as a function of K incorporation for the metallic and insulating phases. This filling is not rigid band–like, and it reflects disorder in the K sites. Theoretical analysis indicates that $K_xC_{60}$ is a strong coupling superconductor, and we suggest that the enhanced electron-phonon interaction is related to the unique hybridization of the C *sp*-derived states.**

SINCE THEIR DISCOVERY (*1*), THE fullerenes have revealed a succession of remarkable properties. These molecules represent the third form of pure C, joining $sp^3$-bonded diamond and $sp^2$-bonded graphite but exhibiting an intermediate form of hybridization of *s*- and *p*-states. For $C_{60}$, the molecular structure is especially symmetric with 60 equivalent atoms in a soccer ball–like configuration (*2, 3*). While these molecules are less stable by 0.4 eV per atom than diamond or graphite (*4*) and they can be burned (*5*), they are exceptionally stable against photofragmentation (*6*). Following the breakthrough in synthesis by Krätschmer *et al.* (*7*), studies of solid-state properties of single crystals of $C_{60}$ have shown that the molecules rotate (*2*) in fcc (face-centered-cubic) lattice sites (*8*) at temperatures well below 300 K. Photoemission and inverse photoemission studies (*9, 10*) have shown a richness in structure for the occupied and empty electronic states of condensed $C_{60}$ and $C_{70}$ as well as a novel molecular plasmon (*9*). First principles calculations have produced good agreement with experiment (*9–12*), and charge delocalization and dispersive band formation have been reported (*10, 11*). Alkali metal incorporation into the fullerite lattice has produced conducting fullerides (*13*). Finally, the discovery of superconductivity (*14*) in $K_xC_{60}$ at 18 K has generated intense interest in the conduction band states and the role of electron-phonon coupling.

This paper focuses on electronic structure changes due to K incorporation in solid $C_{60}$, starting with insulating $C_{60}$, progressing through the metallic state, and reaching the insulating $K_6C_{60}$ state. Photoemission spectra demonstrate the occupancy of ~1-eV wide bands derived from threefold degenerate lowest unoccupied molecular orbitals (LUMOs) of the molecule, but filling is not simply rigid band–like. Instead, the entire LUMO-derived band is evident after low doping, and emission from that band increases with K incorporation. We also observe band broadening associated with disorder in the K bonding sites. In addition, increases in spectral width for the valence band features reflect changes in the crystal field, reduced molecular symmetry, and modification of the band structure. Having identified the band responsible for superconductivity, we provide an estimate of the parameters relevant for superconductivity. From theoretical analysis, we find strong electron-phonon coupling and suggest that *s-p* hybridization in the conduction band is responsible for the increase in coupling compared to intercalated graphite (*4*).

Insight into the likely structure of K-incorporated $C_{60}$ can be gained by analysis of results for K-intercalated graphite (*15*) where the structure can be explained in terms of packing of K ions (ionic radius 1.33 Å) between sheets of C (van der Waals radius 1.68 Å). With these atomic dimensions and the lattice constant of the fcc fullerene, 14.2 Å, it follows that K ions could occupy the interstitial tetrahedral (1.15 Å radius) and octahedral (2.1 Å radius) holes of the fcc lattice. The occupancy of each site by one ion would give a stoichiometry of $K_3C_{60}$. Our total-energy local-density calculations confirm that this is an energetically favored structure since the enthalpy of formation is ~1 eV per K atom (*4*). Fischer and co-workers (*16*) recently reported an x-ray diffraction study of $K_xC_{60}$ grown at 200°C. Their results for the fully reacted equilibrium phase showed a bcc (body-centered-cubic) lattice with K ions occupying tetrahedral sites. The occupancy of each such site would give $K_6C_{60}$ with each anion surrounded by 24 cations. For

---

P. J. Benning, J. L. Martins, J. H. Weaver, Department of Materials Science and Chemical Engineering, University of Minnesota, Minneapolis, MN 55455.
L. P. F. Chibante and R. E. Smalley, Rice Quantum Institute and Departments of Chemistry and Physics, Rice University, Houston, TX 77251.

intermediate stoichiometries, there should be no long-range order in the filling of the various interstitial sites. This absence of periodicity in the K distribution introduces disorder. The ease with which K is taken into the lattice, even at 300 K as in our measurements, indicates relatively easy hopping from one site to the next. The addition of K ions probably impedes molecular rotation (*3*).

For photoemission experiments, phase-pure samples of $C_{60}$ were produced by the contact-arc method with subsequent purification by liquid-phase chromatography (*17*). The resulting powder was degassed in ultrahigh vacuum so that molecules could be sublimed and condensed onto mirror-like GaAs(110) substrates at pressures of $5 \times 10^{-10}$ torr to produce films of 100 Å nominal thickness. Based on scanning tunneling microscopy results for multilayers grown under equivalent conditions (*18*), we expect the surface to exhibit close-packed molecular arrays but with crystalline disorder at grain boundaries. Prior to K deposition, the films were characterized with synchrotron radiation photoemission. They were then exposed to the flux from a well-degassed SAES potassium getter source. The pressure rose to $1 \times 10^{-10}$ torr during K deposition but quickly returned to the operating pressure of $5 \times 10^{-11}$ torr after the source was cooled. The getter source, located ~8 cm from the sample, was heated with a current of 5.8 A. Exposures were timed to produce incremental amounts of K.

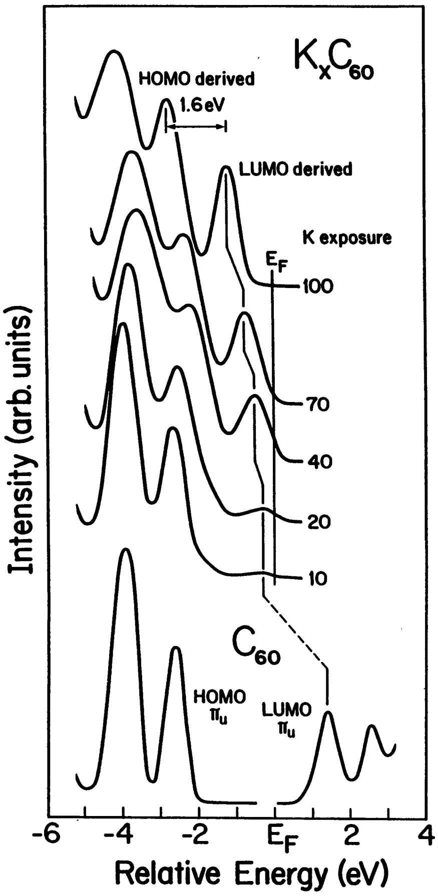

**Fig. 1.** Photoemission spectra for solid $C_{60}$ as a function of K exposure (in timed increments) normalized to the intensity of the largest feature. The bottom curve shows the occupied states of the pure fullerene, together with results for the empty states from inverse photoemission (*10*). All spectra are aligned to the Fermi level. The energies for the molecular solids reflect the removal or addition of an electron when the Fermi level does not lie within a band. K incorporation results in the non–rigid band occupancy of the LUMO-derived states. The metallic state is characterized by the location of $E_F$ within this LUMO-derived band. Continued K incorporation fills the LUMO-derived band, producing the insulating state characterized by the top spectrum.

The bottom left curve of Fig. 1 shows the distribution of occupied electronic states of solid $C_{60}$ measured with photoemission for $h\nu = 65$ eV. The energy reference is the Fermi level ($E_F$) of the spectrometer, 2.6 eV above the peak of the highest occupied molecular orbital (HOMO)–derived band. These results correspond to the molecular solid with one electron removed by photoexcitation. As discussed by Weaver *et al.* (*9*) where the full 20-eV-wide valence bands are shown, the two leading features have C $p_\pi$ bonding character. Mixing of $\pi$ and $\sigma$ character is found in the third major structure, and greater $\sigma$ character is evident in the states farthest from $E_F$ (*9–12*). The empty state features shown in the bottom right curve of Fig. 1 were measured with inverse photoemission (*10*) with an incident electron energy of 17.25 eV. They are referenced to $E_F$ and are scaled so that the threefold degenerate LUMO-derived band is 60% of the fivefold degenerate HOMO-derived band. The energy difference between the LUMO peak and the HOMO peak is the condensed, molecular crystal analog of the difference between the electron affinity level and the ionization potential of the molecule. This difference is 4 eV for the solid, compared to ~5 eV for the free molecule (*19*). According to our local density calculations, the widths of the HOMO- and LUMO-derived bands are 0.84 and 0.64 eV, respectively, and the gap between them is 0.98 eV. These two groups of bands are separated from lower and higher bands by 0.27 and 0.37 eV, respectively. All the gaps are direct at the point X in the Brillouin zone. Curvatures of the LUMO-derived bands indicate that the effective masses are ~2 $m_e$.

The photoemission spectra of Fig. 1 reveal remarkable changes induced by K incorporation. The curve acquired after 10 min of K exposure shows weak emission above the HOMO-derived band. The full width at half maximum of this band is 1.0 eV, and the shape of the leading edge is consistent with a Fermi level cutoff and metallic character, as determined when the scale was expanded. This feature reflects spectral density associated with electrons in the LUMO-derived bands of $K_xC_{60}$. By 30-min exposure, the LUMO-derived feature was stronger but not wider (not shown). By 40-min exposure, the peak had shifted 0.2 eV away from $E_F$, and the intensity was about half of the final intensity. By 70-min exposure, the Fermi level was near the top of the LUMO-derived band, and by 100-min exposure the LUMO bands were entirely below $E_F$. In this insulating stage, the intensity of the LUMO relative to the HOMO was ~0.6. This intensity ratio supports the argument that the threefold degenerate LUMO bands were completely filled; since both bands were $p_\pi$-derived and of odd symmetry, their photoionization cross sections are essentially equal. Moreover, x-ray photoemission studies of $K_xC_{60}$ utilizing substrate level attenuation confirm that saturation occurs at about $K_6C_{60}$.

The appearance of a wide LUMO-derived band after very low K exposure and its growth in intensity with increased exposure is consistent with the above discussion of lattice disorder, K bonding sites, and local concentration differences. In such cases, the spectral density of a given state depends on the local environment (*20*). The resulting behavior is then quite different from that of a rigid band picture in which added electrons simply raise the Fermi level in the bands of the host. It is likely that such disorder cannot be avoided in the alkali fullerides, for the steric reasons discussed above. It should also be noted that the absence of rigid band filling can be explained by the presence of strong electron correlation in the LUMO-derived bands.

The results of Fig. 1 also show significant lineshape changes for the occupied states of the host. In particular, the leading two $p_\pi$ features begin to overlap, as do those at greater binding energy. Moreover, there is substantial broadening of HOMO to lower binding energy, and there is overlap of the HOMO- and LUMO-derived bands. Such effects reflect changes in the crystal field due to the presence of K cations coordinated with $C_{60}$ anions and the reduced symmetry of the molecule. Additional contributions are due to band structure effects since the bands must reflect hybridization with the *s* character of K.

For the pure fullerene, the energy location of the HOMO band relative to $E_F$ is dictated by the ionization potential of the condensed molecule, regardless of the location of the LUMO. Once the molecular LUMO states are partially occupied, however, the molecular solid acts as a metallic solid. As shown in Fig. 1, the energy separation is ultimately 1.6 eV. This is remarkably close to that observed in photoemission from negatively charged $C_{60}$ ions in the gas phase (*21*), despite obvious changes induced by K. The apparent position of the LUMO and HOMO bands again appears too far from $E_F$ when the Fermi level energy reference is no longer pinned to an intrinsic level of the molecular system. This accounts for much of the shift observed between the spectra of Fig. 1 for 70- and 100-min exposures. Examination of the distribution of empty states of $C_{60}$ measured with inverse photoemission (bottom curve) shows that the first and second features are separated by ~1 eV. In the ground state, the conduction band of $K_6C_{60}$ probably lies ~1 eV above the valence band. The fact that no emission is observed above the LUMO-derived bands for 100 min and that the LUMO peak lies far below $E_F$ confirms the picture that an insulating molecular solid is formed after full intercalation with all three LUMO-derived bands occupied. Hence, the stoichiometry is $K_6C_{60}$ for that crystal.

Exposure of a $K_6C_{60}$-based film (characterized by the spectrum for 100-min exposure) to additional K deposition resulted in the nucleation of K metal on the surface. This was reflected by a metallic Fermi level. There were no changes in the valence bands that would indicate that a second unoccupied band was being filled. Annealing of the sample to enhance K intercalation resulted in the elimination of the emission at $E_F$ and a slight sharpening of the valence band features. The inability to force appreciable additional K incorporation is consistent with the filling of all available tetrahedral sites of the bcc lattice (*16*). The addition of more ions of K would start populating the next group of bands of $C_{60}$ which are ~1 eV higher in energy. This would reduce the enthalpy of reaction by the same amount, making it negative so that reaction would be unfavorable.

Finally, the annealed sample was exposed to molecular oxygen in situ. The result was the formation of K-oxide, the leaching of K from the intercalated film, and the loss (to measurements with our surface sensitivity) of emission from the fullerenes. This is consistent with the results of Haddon *et al.* (*13*) that showed severe degradation upon exposure to air.

The results of Fig. 1 explain the changes in conductivity (*13*) and the return to insulating character after complete K incorporation. In the metallic state, they indicate that the conduction band states of $K_xC_{60}$ are C $p_\pi$-derived but are disordered. Insight into the mechanism responsible for superconductivity at 18 K can be gained by comparing the results for $K_xC_{60}$ to those for intercalated graphite (*22*). Superconductivity in the 0.15 to 0.55 K range for $KC_8$, $RbC_8$, and $CsC_8$ and its absence in $LiC_6$ and the higher stage intercalates has been explained by scattering between carbon $\pi$ states and partially occupied cation *s* states (*22*). Electron-phonon scattering within the graphite layers is believed to be too weak to explain the superconducting properties.

From the McMillan equation, a superconducting transition temperature of 18 K in $K_xC_{60}$ would imply that the electron-phonon coupling constant, $\lambda$, would be 0.65 if we assume that the Coulomb pseudopotential is $\mu^* = 0.1$ and the Debye temperature is 700 K. Reasonable assumptions about the range of the Debye temperature and $\mu^*$ lead to values of $\lambda$ between 0.5 and 1.0 such that the system is characterized by strong electron-phonon coupling. For graphite intercalated compounds, the coupling constant is small, $\lambda \sim 0.25$. Since the calculated density of states at the Fermi level is smaller in $K_xC_{60}$ than in intercalated graphite, this implies that the electron-phonon coupling is substantially stronger in the fulleride. In $C_{60}$, the curvature of the bonding network induces *s-p* hybridization in the $\pi$ states (which should more accurately be called mostly-$\pi$ or $\pi$-like states). Such hybridization would enhance the single site matrix elements for electron scattering between two mostly-$\pi$ states by phonons (*4*), and this could explain the stronger coupling and the higher transition temperatures in the fulleride.

REFERENCES

1. H. W. Kroto, J. R. Heath, S. C. O'Brien, R. F. Curl, R. E. Smalley, *Nature* **318**, 162 (1985).
2. R. Taylor, J. P. Hare, A. K. Abdul-Sada, H. Kroto, *J. Chem. Soc. Chem. Commun.* **20**, 1423 (1990); R. Tycko *et al.*, *J. Phys. Chem.* **95**, 518 (1991); C. Yannoni, R. D. Johnson, G. Meijer, D. S. Bethune, J. R. Salem, *ibid.*, p. 9.
3. J. M. Hawkins, A. Meyer, T. A. Lewis, S. Loren, F. J. Hollander, *Science* **252**, 312 (1991).
4. J. L. Martins, N. Troullier, M. C. Schabel, in preparation.
5. For $O_2$-$C_{60}$ interactions, see G. H. Kroll, P. J. Benning, Y. Chen, T. R. Ohno, J. H. Weaver, *Chem. Phys. Lett.*, in press.
6. S. C. O'Brien, J. R. Heath, R. F. Curl, R. E. Smalley, *J. Chem. Phys.* **88**, 220 (1988).
7. W. Krätschmer, L. D. Lamb, K. Fostiropoulos, D. R. Huffman, *Nature* **347**, 354 (1990).
8. R. M. Fleming *et al.*, *Mat. Res. Soc. Symp. Proc.*, in press.
9. J. H. Weaver *et al.*, *Phys. Rev. Lett.* **66**, 1741 (1991).
10. M. B. Jost *et al.*, *Phys. Rev. B*, in press; M. B. Jost *et al.*, in preparation.
11. J. L. Martins, N. Troullier, J. H. Weaver, *Chem. Phys. Lett.*, in press.
12. S. Saito and A. Oshiyama, *Phys. Rev. Lett.* **66**, 2637 (1991); Q. Zhang, J.-Y. Li, J. Bernhole, *ibid.*, p. 2633; J. W. Mintmire, B. I. Dunlap, D. W. Brenner, R. C. Mowrey, C. T. White, *Phys. Rev. B*, in press.
13. R. C. Haddon *et al.*, *Nature* **350**, 320 (1991).
14. A. F. Hebard *et al.*, *ibid.*, p. 600.
15. H. Herold in *Intercalated Materials*, F. Levy, Ed. (Reidel, Dordrecht, 1979), pp. 323–421.
16. O. Zhou *et al.*, *Nature*, in press.
17. R. E. Haufler *et al.*, *Mat. Res. Soc. Symp. Proc.*, in press; *J. Phys. Chem.* **94**, 8634 (1990).
18. Y. Z. Li, J. C. Patrin, M. Chander, J. H. Weaver, L. P. F. Chibante, R. E. Smalley, *Science* **252**, 547 (1991).
19. R. E. Haufler, L.-S. Wang, L. P. F. Chibante, C. Jin, J. Conceicao, Y. Chai, R. E. Smalley, *Chem. Phys. Lett.*, in press.
20. A Bansil and M. Pessa, *Physica Scripta T* **4**, 52 (1983).
21. S. H. Yang, C. L. Pettiette, J. Conceicao, O. Cheshnovsky, R. E. Smalley, *Chem. Phys. Lett.* **139**, 233 (1987).
22. R. Al-Jishi, *Phys. Rev. B* **28**, 112 (1983).
23. This work was supported by the Office of Naval Research, the National Science Foundation, the Robert A. Welch Foundation, and the Minnesota Supercomputer Institute. The measurements were done at the Wisconsin Synchrotron Radiation Center. Stimulating discussions with Y. Chen, M. B. Jost, G. H. Kroll, T. R. Ohno, D. M. Poirier, and N. Troullier are gratefully acknowledged. We thank R. C. Haddon, J. E. Fischer, and their co-workers for sharing results prior to publication.

19 April 1991; accepted 14 May 1991

---

# Photoemission Spectra and Electronic Properties of $K_xC_{60}$

G. K. Wertheim, J. E. Rowe, D. N. E. Buchanan, E. E. Chaban, A. F. Hebard, A. R. Kortan, A. V. Makhija, R. C. Haddon

**Photoemission spectra of vacuum deposited layers of $C_{60}$, before and after exposure to K vapor, show that the K donates its conduction electron into the band derived from the lowest unoccupied molecular orbital. A compound with composition of $K_3C_{60}$, corresponding to the maximum conductivity, has been prepared. In it the potassium atoms presumably occupy both the octahedral and the two tetrahedral interstitial sites of the face-centered-cubic (fcc) $C_{60}$ structure.**

THE DISCOVERY OF NEW METHODS of synthesis of fullerene carbon molecules (*1*) has led to a proliferation of studies of the properties of solid $C_{60}$ (*2–6*). Most of these studies show that the solid form of $C_{60}$ is highly molecular in nature with electronic structure (*2, 3*) that differs little from that of the gas phase molecule.

---

AT&T Bell Laboratories, Murray Hill, NJ 07974.